THE JOURNAL OF PHYSICAL CHEMISTRY B

Article

pubs.acs.org/JPCB

N,N-Dimethyldodecylamine Oxide Self-Organization in the Presence of Lanthanide Ions in Aqueous and Aqueous-Decanol Solutions

Natalia M. Selivanova,*[,†] Aliya I. Galeeva,[†] Andrey A. Sukhanov,[‡] Oleg I. Gnezdilov,[‡] Denis V. Chachkov,[§] and Yury G. Galyametdinov[†,‡]

[†]Kazan National Research Technological University, 68 Karl Marx, Kazan, Russia, 420015

[‡]Zavoisky Physical-Technical Institute, Kazan Scientific Center of Russian Academy of Sciences, 10/7 Sibirskiy Trakt, Kazan, Russia, 420029

[§]Kazan Branch of Joint Supercomputer Center of Russian Academy of Sciences, 2/31 Lobachevskiy, Kazan, Russia, 420111

Supporting Information

ABSTRACT: The article represents the results of research in self-organization of new lanthanide systems in water−decanol medium. The systems are based on *N,N*-dimethyldodecylamine oxide, a zwitterionic surfactant. The study covers the complex formation of lanthanide ions with C_{12}DMAO molecules and the influence of Ln(III) ions and medium composition on surfactant association in diluted solutions. The analysis of adsorption isotherms was carried out on the basis of the combination of Gibbs and Langmuir adsorption equations. The results were used to determine physicochemical properties and parameters of a monomolecular adsorption layer. The research objects were various lanthanide ions with identical coordination centers. A number of spectroscopic methods (UV, NMR self-diffusion, EPR, dynamic light scattering (DLS), and fluorescent analysis) were involved in the research for comparative estimations of molecular dynamics, critical micellization concentration, geometry, sizes, and aggregation numbers of micellar aggregates. Micelle structure simulation revealed good agreement between experimental data and quantum chemical calculations.

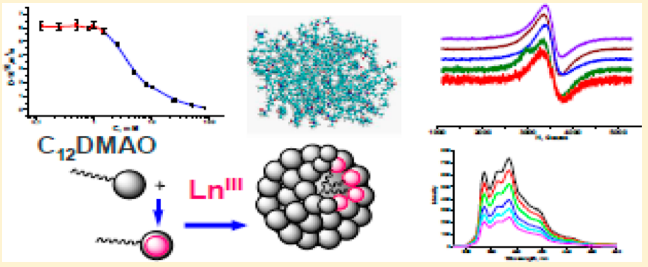

INTRODUCTION

Self-organization of surfactants in solutions attracts strong interest because of its wide application range in various areas of science and technology. Self-assembly of surfactant molecules into micellar structures with specified geometry provides opportunities for design and synthesis of hybrid nanoscale organic/inorganic materials.[1−8] Accuracy of reduplication of self-organization processes provides an accessible control tool for the molecular architecture, size, and geometry of nano-objects.[9,10] This method is based on a biochemical approach similar to the technology of template synthesis of biological materials involving biopolymers and low molecular weight polar lipids as natural origin surface active components.[11,6] The duality of zwitterionic surfactants makes them perfect objects for simulation of biological processes occurring both in micellar state and in more concentrated systems, such as combinations with membrane proteins.[12] Special interest is attracted to the studies of interaction processes of lanthanides in different phase states represented by the aforementioned model systems, as lanthanide ions demonstrate a certain affinity to calcium bonding centers of proteins, membranes, and proteolipids.[13−17] Despite being abiotic, lanthanide ions are popular components of diagnostic systems for their unique optical and magnetic properties. Complex lanthanide compounds are successfully applied as highly efficient luminescent labels and probes for UV (Ce(III) and Gd(III)), visible (Tm(III), Tb(III), Dy(III), Eu(III), and Sm(III)), and near-infrared (Yb(III), Nd(III), Ho(III), and Er(III)) spectral regions[18−20] as well as molecular recognition agents.[21,22] Gadolinium cations are used as contrasting agents for magnetic resonance tomography.[23,24] Our earlier publications were dedicated to research in lanthanides containing C_{12}DMAO-based lyotropic systems, determination of types of forming mesophases, their concentration limits, and phase transition temperatures.[25] Original results were presented for studies in synthesis and nematic mesophase characterization in the C_{12}DMAO/Ln/H_2O/$C_{10}H_{21}OH$ system. The main purpose of the current research was to study the association and complex formation of zwitterionic surfactant molecules and lanthanide ions, the effect of organic additives on self-organization in aqueous media, as well as selection of adequate physicochemical methods for study of micellar solutions. Different physicochemical methods are well-known to provide diverse information for characterization of surface properties and aggregation behavior of surfactant solutions. One of the objectives of the present contribution was to investigate micellization of Ln-containing

Received: January 25, 2013
Revised: March 27, 2013
Published: April 4, 2013

   dx.doi.org/10.1021/jp400875b | *J. Phys. Chem. B* 2013, 117, 5355−5364

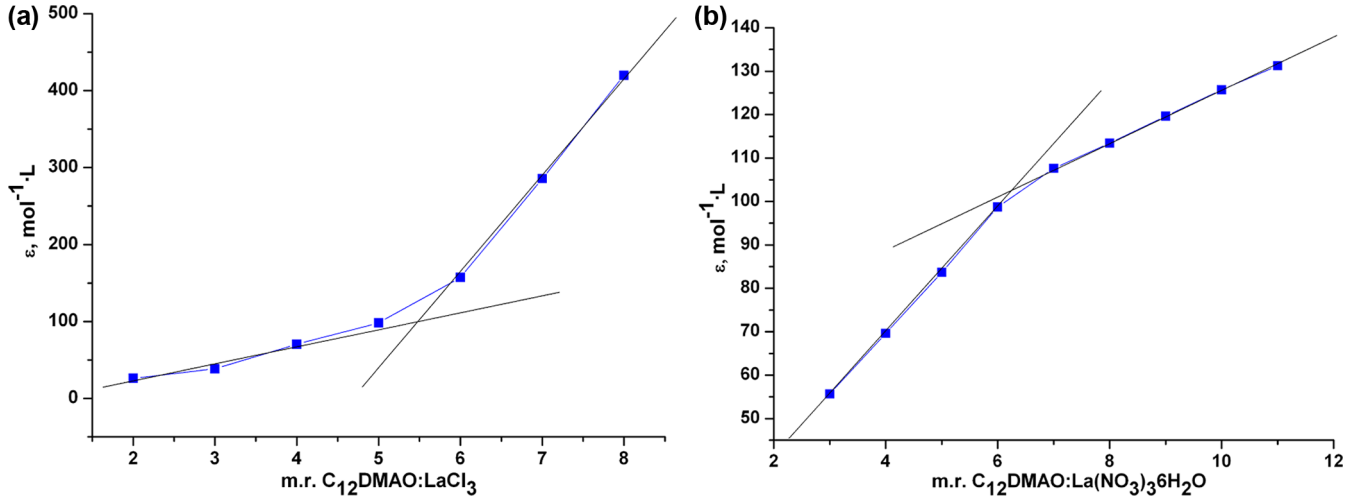

Figure 1. The effect of molar ratios C_{12}DMAO:$LaCl_3 \cdot 5H_2O$ (a) and C_{12}DMAO:$La(NO_3)_3 \cdot 6H_2O$ (b) on the molar extinction coefficient.

surfactant systems by interfacial tensiometry and various spectroscopic methods. Pulsed-gradient spin−echo (PGSE) nuclear magnetic resonance (NMR) was used to determine the structure and molecular dynamics of micelles and monomers. Electron paramagnetic resonance with Gd(III) ions as a spin probe was used for the study of the micelle formation process. Fluorescence probing allowed us to estimate micelle sizes and aggregation numbers in aqueous and aqueous-decanol media. Dynamic light scattering (DLS) was carried out to estimate the approximate size of micellar aggregates and the polydispersity of the systems under study. The results of experiments and quantum chemical calculations were compared to select adequate methods for the study of micellar aggregation.

EXPERIMENTAL SECTION

Materials. Commercial samples of zwitterionic surfactant, *N*,*N*-dimethyldodecylamine oxide $CH_3(CH_2)_{11}N(O)(CH_3)_2$ (C_{12}DMAO), hydrated lanthanide nitrates $La(NO_3)_3 \cdot 6H_2O$, $Gd(NO_3)_3 \cdot 6H_2O$, $Eu(NO_3)_3 \cdot 6H_2O$, lanthanum chloride pentahydrate $LaCl_3 \cdot 5H_2O$ (Ln(III)), decanol $C_{10}H_{21}OH$, pyrene $C_{16}H_{10}$, and cetylpyridinium bromide $C_{21}H_{38}BrN$ (CPB), supplied by "Aldrich", were used for experiments without additional purification.

Solutions were prepared by dissolution of Ln(III) salts in water. The amounts of salts were calculated by the surfactant:Ln(III) molar ratio. Required amounts of surfactants and decanol were added in the next step (the surfactant:$C_{10}H_{21}OH$ = 3.81:1 ratio used for calculation of decanol additives corresponds to decanol amounts used[25] for further preparation of lyotropic mesophases). Solutions were agitated by a magnetic stirrer for 25 min. All the other concentrations were prepared from the initial solution by sequential dilution. Bidistilled water was used as a solvent, and its purity was tested by conductivity (5.5 μS/m) and surface tension (72.5 N/sm^2) methods.

Surface Tension Measurements. Equilibrium surface tension of a system−air interface was measured using the modified Wilhelmy plate method. All the measurements were performed in the thermostatted cell at 25 ± 1 °C.

Dynamic Light Scattering (DLS). The properties of micellar aggregates were studied by dynamic light scattering. A Malvern Zetasizer Nano analyzer was used for the measurements. The source of laser radiation was a He−Ne gas laser with 10 mW power and 633 nm wavelength. The value of the light scattering angle was 173°. Dust removal was accomplished before each measurement with a 0.45 μm Millex HV Filter Unit provided by Millipore.

Ultraviolet (UV) Spectroscopy. UV spectra were taken with a scanning double beam Instrumental Lambda 35 UV/vis Spectrometer by Perkin-Elmer. The measurements were carried out at 25 °C. Quartz cells with 1 cm optical path length were used.

Pulsed-Gradient Spin−Echo (PGSE) Method. The self-diffusion coefficient (D) was measured by an Avance 400 spectrometer (Bruker) with a magnetic field pulsed gradient attachment. The proton resonance frequency value was 400.15 MGz, and the maximum value of the gradient was 0.535 T/m. Self-diffusion coefficients were measured by the PGSE method. The experimental value of the gradient was 0−0.5 T/m assuming constant diffusion times (for every experiment) and the duration of gradient impulses. The diffusion time for every experiment was selected within the range 60−100 ms. D values were determined by the analysis of the diffusion curves representing dependencies of spin−echo integral intensities (obtained by excitation of specific lines in proton NMR spectra) on the square magnetic field gradient.

Electron Paramagnetic Resonance (EPR) Measurement. Stationary EPR spectroscopy was used to study self-organization processes. Spectra were recorded at room temperature with a Bruker EPR EMX/plus spectrometer with ER4122 SHQE resonator. The X-band has been used to measure the EPR spectra.

Fluorescent Analysis. Excitation and fluorescence spectra were obtained using a Varian Cary Eclipse spectrofluorimeter. The pyrene excitation wavelength was λ = 335 nm, while the range of spectra taken was 350−500 nm. Cetylpyridinium bromide was used as a quenching agent. The measurements were taken in a centimeter width quartz cell with a 90° signal registration angle in relation to the excitation light beam. Light filters were used in the automatic mode. The parameters of excitation slit and radiation slits were 20 and 5 nm, respectively.

Computer Simulation. The HyperChem 8.07 software package was used for computer simulation by molecular dynamics[26] with the MM+ method selected for optimization in each point.[27] This method was already tested,[28] it considers potential fields of all system atoms, and it is the most general

dx.doi.org/10.1021/jp400875b | J. Phys. Chem. B 2013, 117, 5355−5364

Table 1. Chemical Shifts (Δ, ppm) of Protons of C_{12}DMAO, C_{12}DMAO-La(III), and C_{12}DMAO/Gd(III) in an Aqueous Solution with C_{Surf} = 8 × 10^{-3} mol/L (TMS as Reference)

chemical group	C_{12}DMAO/H_2O	C_{12}DMAO/La(III)/H_2O	C_{12}DMAO/Gd(III)/H_2O
CH_3 (end group)	0.911	0.925	0.940
$-(CH_2)_9-$	1.329	1.344	1.361
$-N-CH_2-\underline{CH_2}-$	1.821	1.839	1.856
$O-N-(\underline{CH_3})_3$	3.200	3.240	3.248
$-N-\underline{CH_2}-CH_2$	3.308	3.141	3.348

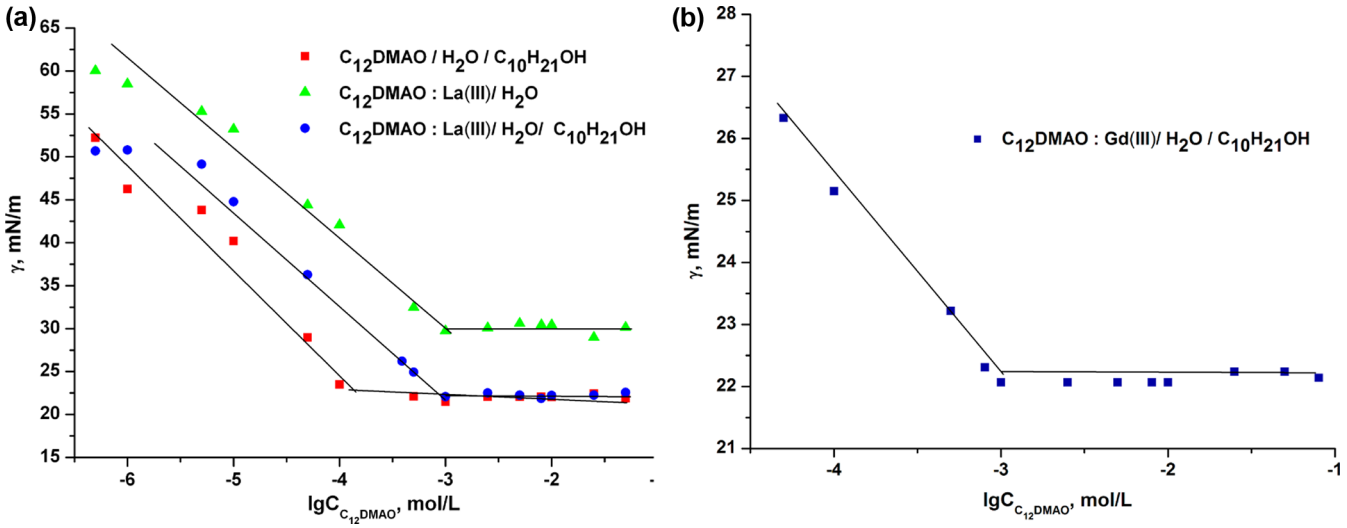

Figure 2. Adsorption isotherms of C_{12}DMAO-based systems in the presence of La(III) (a), Gd(III) (b), and decanol.

tool for all the molecular mechanics methods. Calculations considered the solvent factor in the explicit form: water molecules were assigned around the model structure by the "Periodicbox" procedure in the HyperChem package. This tool places the target structure into a predimensioned cell with a homogeneous distribution of water molecules in a free volume.

RESULTS AND DISCUSSION

Interaction of Lanthanide Ions with C12DMAO in Aqueous Solution. Lanthanum ions in the concentrated liquid crystalline state are capable of complexing with *N,N*-dimethyldodecylamine oxide molecules through intermolecular hydrogen bonding of coordinating ions by oxygen atoms in the molecules of zwitterionic surfactant.[25] In this case, the coordination sphere includes water molecules and a nitro group with bidentate bonding.

Complex formation in aqueous solutions was confirmed by the analysis of electron spectra taken for various C_{12}DMAO:Ln-(III) (1:1 to 11:1) molar ratios. Electron spectra of individual components (in particular, $La(NO_3)_3{\cdot}6H_2O$) demonstrate two bands with $\lambda \sim 200$ nm and $\lambda = 301$ nm absorption maxima. C_{12}DMAO interaction with lanthanum nitrate did not result in the formation of new bands; a more intensive absorption, however, was observed at $\lambda = 301$ nm. Absorption in the 250–325 region corresponds to the $\sigma^* \leftarrow$ n transition,[29] typical for saturated compounds with a lone electron pair, such as La···O–N in this case. Because of possible signal overlapping from lanthanum crystalline hydrate's nitro group, lanthanum chloride $LaCl_3{\cdot}5H_2O$ was used to study interaction of La(III) ions with *N,N*-dimethyldodecylamine oxide. Titration of $LaCl_3{\cdot}5H_2O$ salt by C_{12}DMAO solution was accompanied by a new 265 nm absorption band formation, indicating the $\sigma^* \leftarrow$ n transition, that is, in turn, caused by La–O chemical bonding resulting from C_{12}DMAO–$LaCl_3{\cdot}5H_2O$ interaction. Figure 1 represents the dependence of the extinction coefficient on the C_{12}DMAO:La(III) molar ratio. Inflection points in the curves indicate the formation of a thermodynamically stable complex. ^{1}H NMR experiments provided data for analysis of chemical shifts in the studied binary and triple systems (Table 1).

Comparative analysis of NMR proton spectra of C_{12}DMAO and C_{12}DMAO–La(III) micellar solutions revealed that, in the presence of lanthanum, chemical shifts of resonance signals move to the weaker field area. This effect results from complexing of an oxygen lone electron pair in the organic ligand molecule with an unoccupied orbital of the Ln(III) ion. These effects become more significant in the presence of Gd(III) ion.

The Influence of Ln(III) Ions and Decanol Additives on C_{12}DMAO Micellization. Figure 2 represents surface tension isotherms plotted on the basis of tensiometry data. Classical curves describe the behavior of all studied systems, and curve breaks correspond to CMC values. Adsorption isotherms allow calculating geometrical parameters of micellar aggregates in binary and multicomponent systems. Adsorption capacity was calculated with the Shishkovsky equation (eq 1) combining the Gibbs and Langmuir adsorption isotherm equations for surface tension concentration dependence:

$$\Delta\gamma(b, \Gamma_\infty) = RT\Gamma_\infty \ln(1 - b{\cdot}C) \quad (1)$$

where Γ_∞ is the limiting adsorption. Adsorption equilibrium constant b and Γ_∞ values can be obtained from approximation of the $\Delta\gamma_{exp}-C$ experimental plot in the low concentration range with the least-squares regression method applied to eq 1.

Adsorption layer parameters were calculated from Γ_∞ values, S_0 and δ, where S_0 is the area occupied by one adsorbed

dx.doi.org/10.1021/jp400875b | J. Phys. Chem. B 2013, 117, 5355–5364

Table 2. Surface Activity Characteristics and Adsorption Layer Parameters of C_{12}DMAO-Based Systems

system composition	γ (mN/m)	CMC·10^3 (mol/L)	$\Gamma_\infty \cdot 10^{10}$ (mol/sm^2)	S_0 (Å^2)	δ (Å)	N	R (nm)
C_{12}DMAO/H_2O	37.0 ± 0.5	10	4.50 ± 0.09	36.9 ± 0.8	10.3 ± 0.2	70	1.7
C_{12}DMAO/H_2O/dec	22.8 ± 0.3	0.14	2.77 ± 0.06	60.0 ± 1.3	10.8 ± 0.2	30	2.0
C_{12}DMAO:La(III)/H_2O	29.7 ± 0.4	1	1.63 ± 0.03	102.1 ± 2.1	6.3 ± 0.1	24	1.8
C_{12}DMAO:La(III)/H_2O/dec	22.4 ± 0.3	1	1.85 ± 0.04	110.0 ± 2.3	7.1 ± 0.2	48	1.9
C_{12}DMAO:Gd(III)/H_2O/dec	22.1 ± 0.3	1	1.44 ± 0.03	115.4 ± 2.4	5.5 ± 0.1	40	1.8

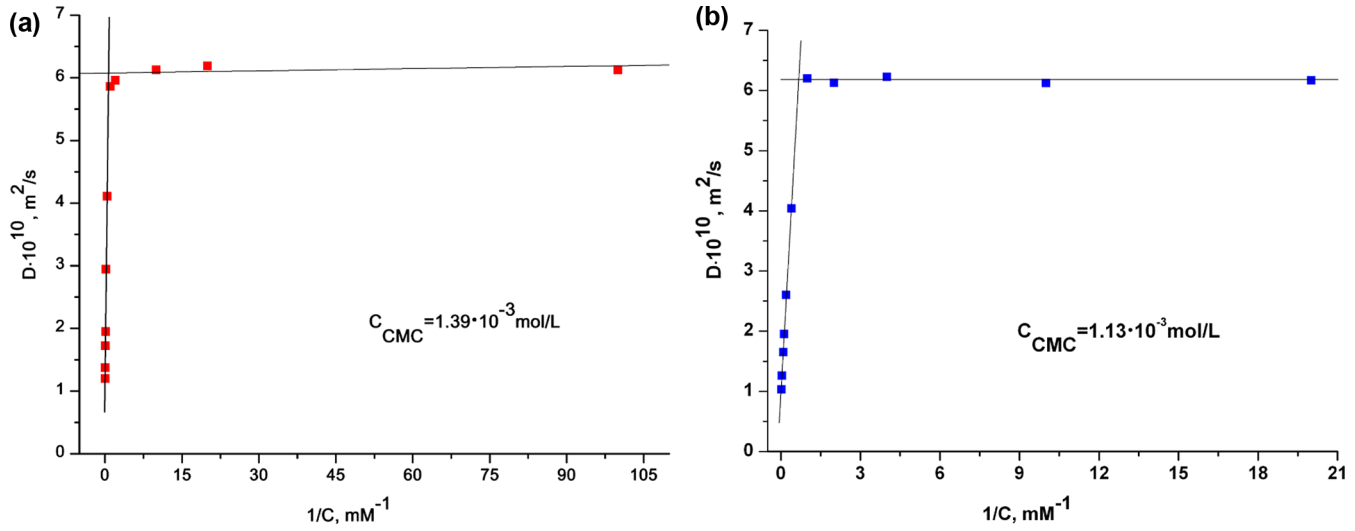

Figure 3. Self-diffusion concentration dependence for the C_{12}DMAO:La(III)/H_2O (a) and C_{12}DMAO:La(III)/H_2O/dec (b) systems.

molecule equal to the area of its polar hydrophilic part and δ is the thickness of an adsorption layer. Equation 3 assumes that the molecules are adsorbed at the interface in a vertical conformation:

$$S_0 = \frac{1}{\Gamma_\infty \cdot N_A} \quad (2)$$

$$\delta = \frac{M \cdot \Gamma_\infty}{\rho} \quad (3)$$

Surface tension isotherms provided data for calculation of aggregation numbers (N) by the Rusanov[30] method.

Addition of Ln(III) ions reduces surface tension γ values and lowers the CMC in the range of 1 order of magnitude compared with the basic C_{12}DMAO/water system. Addition of electrolytes to nonionic surfactant solutions reduces the CMC as the result of the salting out effect.[31,32] The complexing process increases system polarizability in the case of systems under study through ion−dipole interactions of Ln ion and polar groups of surfactant molecules and decrease of their hydration degree followed by CMC reduction. These data are in agreement with our previous studies,[25,33] where this effect was observed for nonionic surfactants.

Addition of decanol to a basic water/surfactant system is accompanied by 14 N/m reduction of surface tension and CMC shifts to 2 orders of magnitude lower area as well. Such a significant change of C_{12}DMAO surface activity is caused by a cosurfactant effect of 3.8 mol of decanol additives resulting in a mixed micellization process and respective increase of hydrophobic effect.

However, addition of decanol to triple C_{12}DMAO/Ln(III)/H_2O systems does not provide a substantial synergetic effect. Ln(III) ions do not exert an influence on the σ value, so it remains at the level typical for C_{12}DMAO/H_2O/$C_{10}H_{21}OH$ systems, while CMCs of metal-containing systems do not change in the presence of decanol.

Table 2 summarizes the main adsorption parameters of studied systems and the sizes of micellar aggregates assuming a spherical shape of particles.

The micellar structures described in Table 1 are characterized by much lower values of S_0 area (the area occupied by a single adsorbed molecule and equal to the area of the hydrophilic group of a surfactant molecule) in binary C_{12}DMAO/H_2O systems than of micelles formed involving lanthanide ions. As it was mentioned before, lanthanide ion can coordinate up to six surfactant molecules, thus increasing the size of the molecule's polar segment. Added decanol molecules penetrate into spherical micelles and contribute to enlargement of hydrophilic molecular segments as well. It was proven in ref 34 that decanol can interact with polar parts of surfactant molecules (1-hexadecyl-3-methylimidazolium chloride) through hydrogen bonding and increase their volume. For metal-containing systems, intermolecular hydrogen bonding is possible involving coordination of Ln(III) ions with alcohol oxygen atom and resulting growth of the polar segment caused by steric factor.

The behavior of adsorption layer (δ) thickness is not smooth; this parameter decreases in systems containing decanol and Ln(III) ion. As the presence of a metal ion in the system does not exert a significant influence on a surfactant's hydrocarbon radical conformation, the δ decrease can be explained by the favored inclined orientation of nonpolar fragments in the adsorption layer. Compared to the basic surfactant/water system, the series of studied multicomponent systems reveals a decrease of aggregation numbers (n) being in agreement with the growth of hydrophilic segments.

The Study of Self-Organization Processes by Spectroscopic Data Analysis. *NMR Self-Diffusion.* The nuclear

dx.doi.org/10.1021/jp400875b | J. Phys. Chem. B 2013, 117, 5355−5364

magnetic resonance relaxation method is an efficient and informative tool for study of molecular motions in micellar systems. The analysis of NMR self-diffusion data is mainly based on a simplified two-state model.[35,36] According to this model, surfactant molecules are in the monomer state at concentrations far below the CMC, while the increase of concentration is followed by their aggregation into the bound, micellar state. Determination of self-diffusion coefficient (D) within the tens of milliseconds range is carried out in fast molecular exchange conditions because the surfactant molecule lifetime in a micelle is within 10^{-5}–10^{-7} s.[37] Thus, the observed D values express the weight average of monomer and micellar diffusion mobilities:

$$D_{obs} = p_f D_f + p_m D_m \quad (4)$$

where p_f and p_m are the molar parts of monomer (free) and micellar surfactant molecules, respectively, and D_f and D_m are self-diffusion coefficients of monomer and micellar surfactant molecules, respectively.

Correlation between molar parts, monomer c_f, micellar c_m, and total c_t surfactant concentrations is expressed by the following equation:

$$p_f + p_m = 1, \quad p_f = \frac{c_f}{c_t}, \quad p_m = \frac{c_m}{c_t} \quad (5)$$

Modification of eqs 4 and 5 leads to an expression for monomer surfactant concentration:

$$c_f = c_t - c_m = c_t \frac{D_{obs} - D_m}{D_f - D_m} \quad (6)$$

Figure 3 represents the concentration dependences of C_{12}DMAO molecules D in diluted solutions with added decanol and lanthanum ions.

The concentration dependence contains two fragments where D values are constant within the experimental error and thus correspond to the monomer state of C_{12}DMAO molecules. Lower D values are observed in the lower concentration range, indicating molecular structural transformations, when surfactant molecules change their state in solution due to micellization. The two-state model assumes the CMC to be the intersection of two linear fragments in $D - 1/C$ coordinates.

The obtained concentration dependence of surfactant D values can be adequately described in terms of the two-state model and eq 4. $D_{obs} = D_f$ for infinitely dilute solutions with no micelles. The micellization process in the above CMC concentration range leads to an increase of the number of micelles, while the concentration of free surfactant molecules stays almost constant. This process is accompanied by a rapid drop of D_{obs} values tending to D_m in the extreme case and depending on the total surfactant concentration and the size of micelles. This effect is confirmed by Figure 4 data comparing contributions of monomer (curve 1) and micellar (curve 2) molar fractions of surfactant to its total concentration.

CMC values of studied systems are summarized in Table 3 and are in good agreement with tensiometry data. Addition of decanol leads to a slight change of D values, thus confirming mixed micellization. Calculations carried out by the Einstein–Stokes equation prove that the size of aggregates increases as well.

EPR Spectroscopy. EPR spectroscopy, such as spin probe EPR, is a unique instrument for studying molecular dynamics

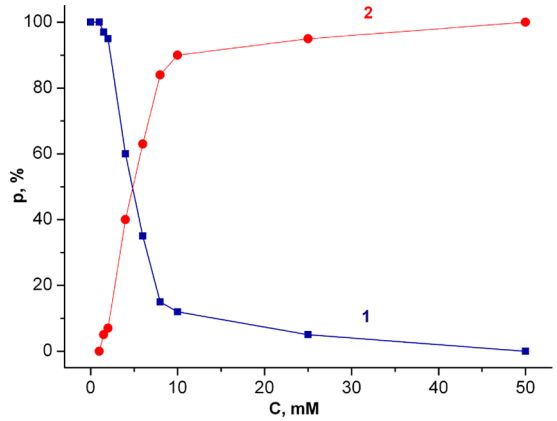

Figure 4. Dependence of the molar fraction of C_{12}DMAO individual molecules (curve 1) and C_{12}DMAO molecules in micelles (curve 2) on surfactant concentration in the C_{12}DMAO:La(III)/H_2O system at T = 298 K.

and structures of micellar systems as well as processes of metal ion binding with proteins and peptides in micellar systems being the models of membrane-mimic systems.[38–41] As a micelle is a complex microheterogeneous system, it is of principal importance to consider localization of labels in a micelle if spin probes are used.[38] We studied association in multicomponent systems containing Gd(III) ions because they have the longest relaxation time of all lanthanide ions (10^{-9}–10^{-10} s). In addition, Gd(III) ion is a structural complexing component and is a priori incorporated into micelles, thus offering advantages for EPR studies.

Figure 5a represents EPR spectra of C_{12}DMAO:Gd(III)/H_2O/$C_{10}H_{21}OH$ solutions in the 8×10^{-3} to 1×10^{-1} mol/L concentration range. The spectra contain a wide singlet in the studied concentration range.

The radius of the micelles (R) was calculated by the Einstein–Stokes equation assuming that micelles are of spherical geometry:

$$R = \sqrt[3]{\frac{3kT\tau_c}{4\pi\eta}} \quad (7)$$

where τ_c is the rotation correlation time, k is the Boltzmann constant, T is the absolute temperature, and η is the water viscosity.

The rotation correlation time was obtained from EPR spectra and the ratio[42]

$$\tau_c = \frac{5}{32}\frac{\Delta H}{\overline{D{:}D}} \quad (8)$$

where ΔH is the EPR line width and the $\overline{D{:}D}$ parameter is calculated using the equation

$$\overline{D{:}D} = \frac{3}{2}D^2 + 2E^2 \quad (9)$$

where D and E are the fine structural parameters characterizing local crystalline field symmetry on a gadolinium ion.

According to eq 7 based calculations, the radius of micelles (R) in aqueous-decanol C_{12}DMAO solutions is about 1.5 nm in the presence of Gd(III) ions with no significant changes in the studied concentration range.

Comparison of aqueous-decanol systems (Table 4) reveals close values of micellar aggregates. Correlation of these results

dx.doi.org/10.1021/jp400875b | J. Phys. Chem. B 2013, 117, 5355–5364

Table 3. Self-Diffusion Coefficients of C_{12}DMAO Molecules in Multicomponent Systems and Respective Micellization Parameters

system	monomer D, D_f (10^{-10} m^2/s)	micellar D, D_m (10^{-10} m^2/s)	CMC·10^3 (mol/L)	radius of micelles, R_h (nm)
C_{12}DMAO:La(III)/H_2O	6.10	1.18	1.39	2.08
C_{12}DMAO:La(III)/H_2O/dec	5.35	0.45	1.13	5.44
C_{12}DMAO:Gd(III)/H_2O	6.20	1.03	1.47	2.38
C_{12}DMAO:Gd(III)/H_2O/dec	6.10	0.41	1.72	5.86

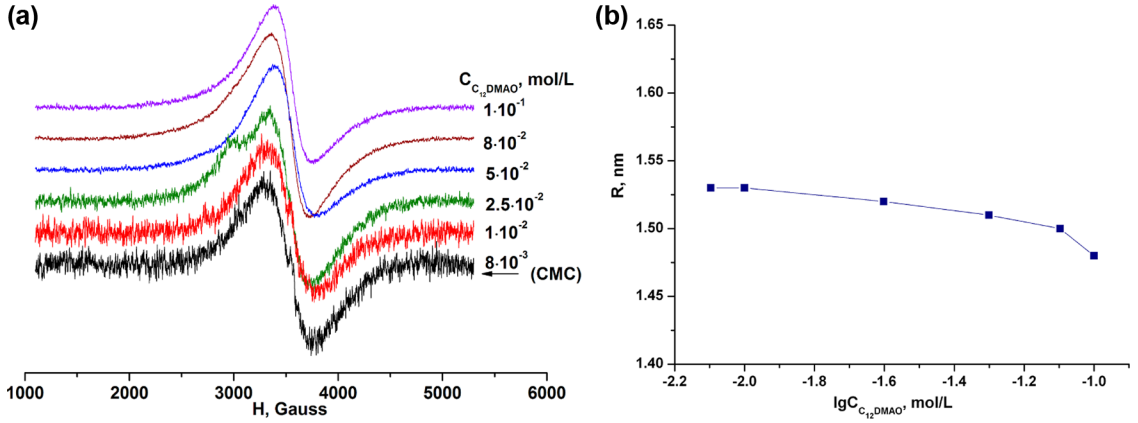

Figure 5. EPR spectra of C_{12}DMAO:Gd(III)/H_2O/$C_{10}H_{21}OH$ aqueous solutions at T = 300 K at various concentrations (a) and the sizes of aggregates calculated from these spectra (b).

Table 4. Rotation Correlation Times and Sizes of Micellar Aggregates

system	C·10^2 (mol/L)	τ_c (ns)	R (nm)
C_{12}DMAO: Gd(III)/H_2O	5	1.19	1.10
C_{12}DMAO: Gd(III)/H_2O	1	1.45	1.17
C_{12}DMAO: Gd(III)/H_2O/dec	5	1.10	1.07
C_{12}DMAO: Gd(III)/H_2O/dec	1	1.60	1.21

with tensiometry and NMR self-diffusion data leads to a conclusion that EPR data describe in this case the size of coordination environment closest to the paramagnetic center which is a Gd(III) ion.

DLS Method. The DLS method was used for detailed study of the sizes of micellar aggregates in a wide concentration range for C_{12}DMAO solutions and in the presence of decanol and lanthanide ions (Figure 6).

DLS data allow tracking of general tendencies in the behavior of C_{12}DMAO aggregates in the presence of various additives. In general, all the studied systems in aqueous and aqueous-decanol media are polydisperse. Polydispersity index (PI) values are the following: $PI_{C_{12}DMAO/H_2O}$ = 0.464, $PI_{C_{12}DMAO/La(III)/H_2O}$ = 0.634, and $PI_{C_{12}DMAO/La(III)/H_2O/dec}$ = 0.637. The found PI values for binary systems as well as for multicomponent systems are above 0.2, which indicates a polydisperse character of micellar solutions. Comparative analysis of surfactant/water systems demonstrates that, in the presence of decanol, the average increase of the size of aggregates is 3 nm. The approximate value of the effective hydrodynamic radius of aggregates D_h is 5−6 nm, as the result of mixed micellization. A similar tendency of constant micellar aggregate size can be observed in these systems when the surfactant concentration increases in the range (1−8) × 10^{-2} mol/L.

It was possible to register the formation of aggregates in the CMC range for lanthanide-containing systems C_{12}DMAO/La(III)/H_2O. A bimodal distribution of aggregates with ∼2.0 and 5.6 nm sizes was observed at C_{CMC} = 1 × 10^{-3} mol/L (Figure S2, Supporting Information). The concentration range of (1−8) × 10^{-2} mol/L is characterized by steady growth of aggregate sizes with the increase of surfactant concentration both for systems containing lanthanum ions and for multicomponent systems with decanol C_{12}DMAO/La(III)/H_2O/dec. The size of micelles is 5−7 times larger than in the basic surfactant/water system when a concentration of 8 × 10^{-2} mol/L is achieved. The presence of surfactant-coordinated lanthanum ion and free NO_3^- counterions favors intensification of dipole−dipole interactions performed by both water molecules and surfactant polar groups, thus increasing the micellar aggregate's solvation shell. This effect becomes more significant with the increase of surfactant concentration.

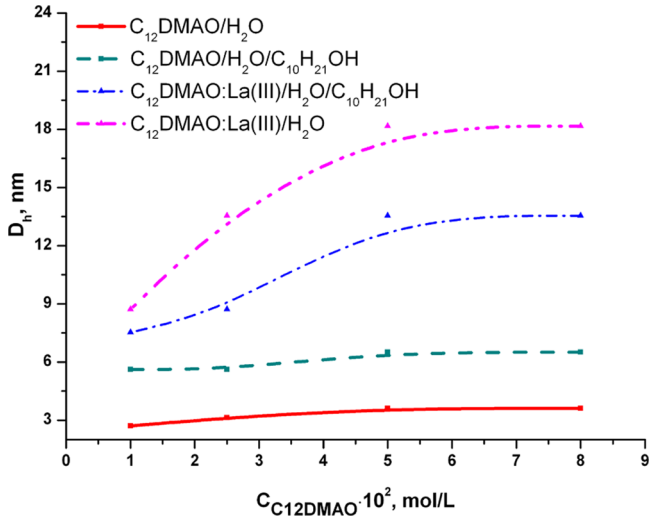

Figure 6. Concentration dependences of the sizes of aggregates (T = 300 K).

dx.doi.org/10.1021/jp400875b | J. Phys. Chem. B 2013, 117, 5355−5364

Fluorescent Analysis. The fluorescence method with pyrene as a luminescent probe was used to study the influence of Ln(III) ions and decanol additives on self-organization in zwitterionic surfactant solutions. Aggregation numbers were determined by the spectrophotometry method described in the literature.[43,44] This method is based on stationary fluorescence quenching measurements and is a reliable tool for determination of micellar aggregation numbers. The oscillating structure of luminescence spectra is highly sensitive to changes in the immediate environment of complexes; this effect is especially intensive for pyrene, allowing its efficient application as a fluorescent probe, for example, for measuring CMC and aggregation numbers.[45−48]

Figure 7 represents the following example: a concentration dependence of pyrene signal intensities ratio I_1/I_3 in the

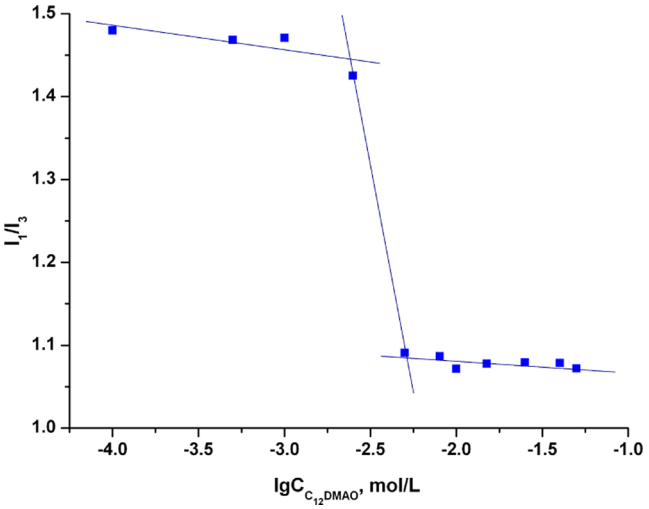

Figure 7. Concentration dependence of I_1/I_3 pyrene fluorescence intensity ratios in the $C_{12}DMAO/H_2O$ system using pyrene additives.

$C_{12}DMAO/H_2O$ system ($C_{C_{12}DMAO}$ = 1 × 10^{-6} to 5 × 10^{-2} mol/L, C_{pyrene} = 1 × 10^{-6} mol/L). The ratio of the first and third peaks characterizes the polarity of the probe's surrounding environment and can be used to estimate micelle hydrophobicity.[49] When CMC concentration is reached, probe redistribution occurs in a solution, therefore leading to rapid change of probe environment parameters. Abrupt decrease of the I_1/I_3 ratio is caused by transition from monomer surfactants to micelles.

All studied systems demonstrate similar behavior. Table 5 represents CMC values obtained from curve breaks. All the data are within one decimal order and agree with tensiometry and NMR results. They reflect the general tendency of CMC decrease in the presence of decanol and lanthanide ions compared with the binary $C_{12}DMAO/H_2O$ system without additives. It should be noted that the fluorescent analysis method proved to be more sensitive to the type of lanthanide ion forming aggregates in multicomponent systems than tensiometry. The system with Gd(III) ion is characterized by the lowest CMC value. Simultaneous presence of lanthanide ion and decanol provides an antagonistic effect. It is possibly caused by different mechanisms influencing the CMC: the properties of decanol as a cosurfactant make it capable of forming mixed micelles, thus achieving a direct increase of the hydrophobic effect, while lanthanide ion forms complexes with amine oxide and reduces the hydration degree of polar surfactant groups. It should be noted that these effects are confirmed by the change of pyrene polarity parameter (I_1/I_3) and resulting formation of more hydrophobic micelles in the presence of decanol.

Table 5. CMC Values, Aggregation Numbers, and the Sizes of Micelles Based on Fluorescent Quenching Data

system composition	CMC·10^3 (mol/L)	I_1/I_3	N_{agg}
$C_{12}DMAO/H_2O$	4.00	1.28	79
$C_{12}DMAO/H_2O$/Dec	0.87	1.24	49
$C_{12}DMAO$:La(III)/H_2O	1.70	1.26	56
$C_{12}DMAO$:Gd(III)/H_2O	0.77	1.26	59
$C_{12}DMAO$:La(III)/H_2O/Dec	1.78	1.24	50
$C_{12}DMAO$:Gd(III)/H_2O/Dec	1.00	1.24	31
$C_{12}DMAO$:Eu(III)/H_2O/Dec	1.62	1.24	47

Luminescence of the $C_{12}DMAO/H_2O$ and $C_{12}DMAO/H_2O$/Dec systems was studied for estimation of aggregation numbers. Measurements were carried out in the presence of pyrene and various concentrations of cetylpyridinium bromide (a quenching agent with C = (1−8) × 10^{-5} mol/L).

Aggregation numbers were determined according to eq 10:

$$\ln \frac{I_0}{I} = \frac{[Q]N_{agg}}{[C] - [CMC]} \quad (10)$$

where I and I_0 are the intensities of fluorescence with a quenching agent and without it, respectively, [Q] is the quenching agent concentration, [C] is the surfactant concentration, and [CMC] is the critical micellization concentration. Variation of fluorescence intensity at different concentrations of a quenching agent and constant surfactant concentration ($C_{C_{12}DMAO}$= 5 × 10^{-3} mol/L) makes it possible to obtain aggregation numbers from $\ln(I_0/I) = f([Q])$ line slopes, according to eq 10.

This method is based on the following assumptions: probe and quenching agent molecules are solubilized in micelles. A single quenching molecule in a micelle deactivates all solubilized probe molecules. The residence time of the fluorescent molecule and the quencher inside the micelle is longer than the unquenched lifetime of the fluorescent probe. Distributions of probe and quencher in micelles obey Poisson statistics.[44]

Figure 8 demonstrates pyrene fluorescence spectra (a) and the linear dependence I_0/I in Stern−Volmer coordinate for various quenching agent concentrations (b).

The analysis of aggregation numbers (Table 5) reveals their decrease for a series of studied multicomponent systems in comparison with the $C_{12}DMAO/H_2O$ system. This effect agrees with tensiometry data, while the obtained value N_{agg} = 79 for a binary $C_{12}DMAO/H_2O$ system is in agreement with literature data.[12,50] The aggregation number N_{agg} = 70 is typical for surfactant molecules with 12 CH_2 groups in a hydrocarbon chain in a near-CMC range.

The data confirm that introduction of decanol into a binary system decreases aggregation numbers due to alcohol penetration into spherical micelles and mixed micellization. This effect was observed for additives of linear alcohols, such as butanol, pentanol, and hexanol to micellar systems of dimeric cationic surfactants.[49] Lower values of aggregation numbers N_{agg} indicate the formation of micelles with a lower density of packing than in pure aqueous solutions. It favors easier

dx.doi.org/10.1021/jp400875b | J. Phys. Chem. B 2013, 117, 5355−5364

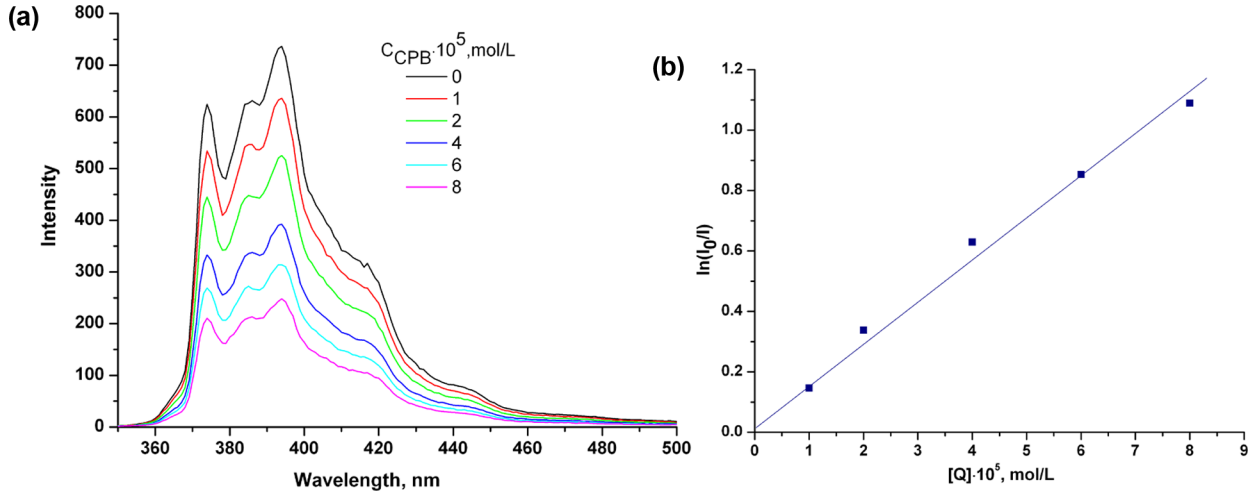

Figure 8. Effect of quenching agent (cetylpyridinium bromide) concentration on pyrene fluorescence intensity: spectra (a) and $\ln(I_0/I)$ vs Q (b) for C_{12}DMAO in aqueous micellar solution ($C(C_{12}DMAO) = 1 \times 10^{-2}$ mol/L, C(pyrene) = 1×10^{-6} mol/L).

penetration of alcohol molecules.[49] Decrease of micellar aggregation numbers caused by addition of polar organic solvents can be generally explained by reduction of interfacial Gibbs energy. Observed differences in CMC values for systems containing La(III) and Gd(III) can be explained by various polarizabilities of ions, determined by their electron structure. The ionization potential of La(III) is 36.5 eV, while this value for Gd(III) is ~40.2 eV.[51] Ionic interactions of the Gd ion with the polar groups of surfactant become more intensive in this case, and the degree of hydration of these groups decreases. This results in a more significant CMC reduction.

Computer Simulation. A spherical micelle with 70 C_{12}DMAO molecules was the initial model system selected on the basis of the experimental data (Figure 9a). The results of computer simulation carried out for the gas phase without consideration of water molecules are summarized in Figure 9b. Calculation results confirm that the structure of the micellar aggregate is mostly spherical with inward hydrocarbon tails and outward polar groups. The radius of the simulated structure is approximately 2.2 nm, that is, in satisfactory agreement with tensiometry data.

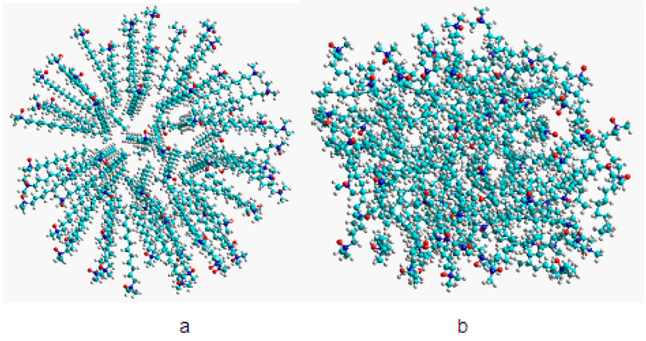

Figure 9. Spherical micelle simulation: (a) initial structure; (b) molecular dynamics results.

A more accurate model was created by the "Periodicbox" procedure in the HyperChem package. According to this procedure, the micelle of C_{12}DMAO molecules is placed inside a 5.7 nm cell with uniform distribution of water molecules in the free volume (Figure 10a). Molecular dynamics optimization was carried out for T = 300 K and 3922 water molecules in a cell. Calculations (Figure 10b) confirm the existence of a sustainable spherical micellar structure. The internal micellar core is formed by hydrophobic parts of diphilic molecules, while the surface layer consists of surfactant polar groups hydrated by water molecules.

CONCLUSION

The influence of Ln(III) ions and decanol additives on self-organization processes in zwitterionic surfactant solution was analyzed in this contribution. Spectrophotometric titration results confirm complexing of lanthanum ions with C_{12}DMAO molecules. This phenomenon leads to a change of surfactant properties: a decrease of surface tension and CMC value is observed. Solution–air adsorption layer parameters were analyzed. It was proven that the presence of lanthanide ions leads to a significant increase of the surfactant molecule's polar part, so complexing of Ln(III) ions with amine oxide's oxygen is, therefore, confirmed. Comparison of the aforementioned parameters with characteristics of the surfactant/water binary system leads to the conclusion that coordination of several surfactant molecules is possible. These results are in agreement with spectrophotometric titration data.

Decanol additives with a molar ratio of 3.8 increase the surface activity of C_{12}DMAO: the CMC drops by 2 orders of magnitude, thus confirming the decanol effect as a cosurfactant. Additional interfacial adsorption of decanol and its participation in mixed micellization make a significant contribution to decrease the interfacial surface energy.

The set of spectroscopic methods was selected for study of self-organization processes and estimation of the size of micelles. Table 6 summarizes comparative data of micelle sizes obtained from adsorption values and the results of spectroscopic methods.

Various physicochemical methods provide different values for effective sizes of micellar aggregates. Calculation of micellar radius by tensiometry applies the adsorption layer model with a micellar aggregate as a spherical hollow-free compact hydrocarbon core with no solvation shells taken into consideration. Size effects arise only if the size of the micelles is significant. However, analysis of adsorption isotherms for calculation of adsorption layer parameters is also an appropriate tool for a

dx.doi.org/10.1021/jp400875b | J. Phys. Chem. B 2013, 117, 5355–5364

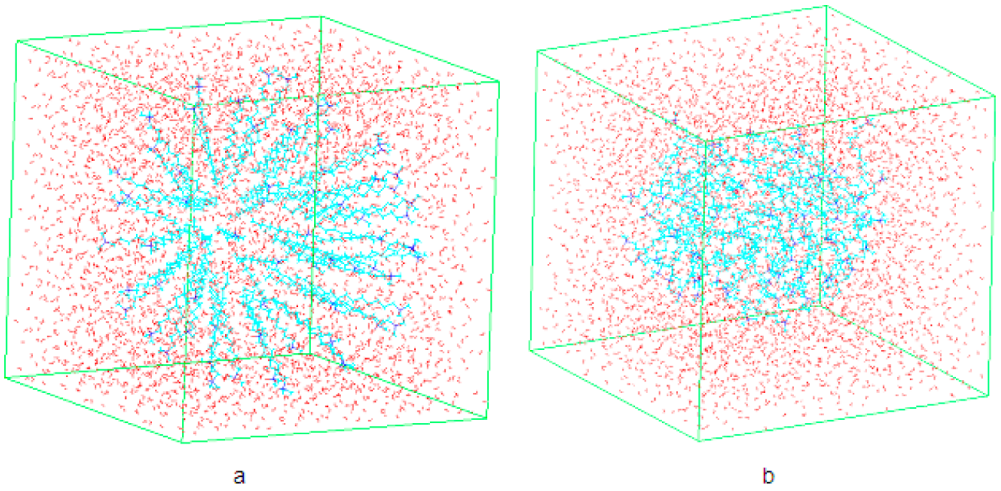

Figure 10. Spherical micelle simulation with solvent molecules: (a) initial structure; (b) the structure after molecular dynamics calculations (10 ps interval with 0.001 ps steps).

Table 6. The Sizes of Micellar Aggregates at C_{CMC} Based on Data from Various Research Methods

	tensiometry	DLS	NMR	fluorescence
system composition	R (nm)	R (nm)	R (nm)	R (nm)
$C_{12}DMAO/H_2O$	1.70	1.6		1.8
$C_{12}DMAO/H_2O$/dec	1.51	3.1		3.1
$C_{12}DMAO$:La(III)/H_2O	1.50	2.5	2.08	3.2
$C_{12}DMAO$:La(III)/H_2O/dec	1.49	3.6	5.44	3.3
$C_{12}DMAO$:Gd(III)/H_2O	1.50	2.1	2.38	3.1
$C_{12}DMAO$:Gd(III)/H_2O/dec	1.54	4.3	5.86	4.3
$C_{12}DMAO$:Eu(III)/H_2O/dec	1.52	5.0		1.9

thorough study of lanthanide ion interactions with amine oxide molecules.

Spectroscopic methods used for estimation of micelle size are based on the measurements of aggregate diffusion with rotational and translational components of a micelle as an integral entity, where micelle dynamics is determined by its external size with solvation shell taken into consideration. This is the main reason why NMR self-diffusion and DLS results demonstrate larger sizes of micelles than tensiometry data. However, spectroscopic methods are sensitive to the composition of systems and can, therefore, track changes of micellar aggregate size caused by lanthanide ions and decanol additives. A possible interpretation of EPR data can be done in terms of their correspondence to the volume of the paramagnetic center surrounding environment. Good correlation between experimental data and computer simulation results confirms the appropriateness of such an approach for simulation of a micellar aggregate.

■ ASSOCIATED CONTENT

Supporting Information

Self-diffusion concentration dependence for the $C_{12}DMAO$:Gd(III)/H_2O (a) and $C_{12}DMAO$:Gd(III)/H_2O/dec (b) systems (Figure S1); size distribution for the $C_{12}DMAO$:La(III)/H_2O systems at different concentrations (Figure S2). This material is available free of charge via the Internet at http://pubs.acs.org.

■ AUTHOR INFORMATION

Corresponding Author

*E-mail: natsel@mail.ru.

Notes

The authors declare no competing financial interest.

■ ACKNOWLEDGMENTS

The work was supported by the Russian Foundation for Basic Research (Project No. 11-03-00679-a)

■ REFERENCES

(1) Zhifeng, B.; Timothy, P. Pluronic Micelle Shuttle between Water and an Ionic Liquid. *Langmuir* **2010**, *26*, 8887−8892.

(2) Qiao, Y.; Lin, Y.; Wang, Y.; Li, Z.; Huang, J. Controllable Synthesis of Water-Soluble Gold Nanoparticles and Their Applications in Electrocatalysis and Surface-Enhanced Raman Scattering. *Langmuir* **2011**, *27*, 1718−1723.

(3) McLeod, M. C.; McHenry, R. S.; Beckman, E. J. Solvent Effects on the Growth and Steric Stabilization of Copper Metallic Nanoparticles in AOT Reverse Micelle Systems. *J. Phys. Chem. B* **2003**, *107*, 2693−2700.

(4) Gröschel, A. H.; Schacher, F. H.; Schmalz, H.; Borisov, O. V.; Zhulina, E. B.; Walther, A.; Müller, A. H. E. Precise Hierarchical Self-Assembly of Multicompartment Micelles. *Nat. Commun.* **2012**, *3*, 1−10.

(5) Jeong, Y. H.; Yoon, H.-J.; Jang, W.-D. Dendrimer Porphyrin-Based Self-Assembled Nano-Devices for Biomedical Applications. *Polym. J.* **2012**, *44*, 512−521.

(6) McHale, R.; Patterson, J. P.; Zetterlund, P. B.; Rachel, K. Biomimetic Radical Polymerization via Cooperative Assembly of Segregating Templates. *Nat. Chem.* **2012**, *4*, 491−497.

(7) Li, Z.; Ma, R.; Li, A.; He, H.; An, Y.; Shi, L. Intensity-Tunable Micelles and Films Containing Bimetal Ions-Europium(III) and Terbium(III). *Colloid Polym. Sci.* **2011**, *289*, 1429−1435.

(8) Zhu, J. Y. Y.; Wang, L.; Peng, M.; Tong, S.; Cao, X.; Qiu, H.; Xu, X. Enhancement of Oral Bioavailability of the Poorly Water-Soluble Drug Silybin by Sodium Cholate/Phospholipid-Mixed Micelles. *Acta Pharmacol. Sin.* **2010**, *31*, 759−764.

(9) Holmberg, K. J. Surfactant-Templated Nanomaterials Synthesis. *J. Colloid Interface Sci.* **2004**, *274*, 355−364.

(10) Lisiecki, I. Size, Shape, and Structural Control of Metallic Nanocrystals. *J. Phys. Chem. B* **2005**, *109*, 12231−12244.

(11) Holmberg, K.; Jönsson, B.; Kronberg, B.; Lindman, B. *Surfactants and Polymers in Aqueous Solution*; John Wiley & Sons, Ltd.: Chichester, England, 2003.

(12) Timmins, P. A.; Hauk, J.; Wacker, T.; Welte, W. A Physical Characterization of Some Detergents of Potential Use for Membrane Protein Crystallization. *FEBS Lett.* **1991**, *280*, 115−120.
(13) Vuojola, J.; Syrjänpää, M.; Lamminmaki, U.; Soukka, T. Genetically Encoded Protease Substrate Based on Lanthanide-Binding Peptide for Time-Gated Fluorescence Detection. *Anal. Chem.* **2013**, *85*, 1367−1373.
(14) Corson, D. C.; Williams, T. C.; Sykes, B. D. Calcium Binding Proteins: Optical Stopped-Flow and Proton Nuclear Magnetic Resonance Studies of the Binding of the Lanthanide Series of Metal Ions to Parvalbumin. *Biochemistry* **1983**, *22*, 5882−5889.
(15) Karhunen, U.; Rosenberg, J.; Lamminmäki, U.; Soukka, T. Homogeneous Detection of Avidin Based on Switchable Lanthanide Luminescence. *Anal. Chem.* **2011**, *83*, 9011−9016.
(16) Niedzwiecka, A.; Cisnetti, F.; Lebrun, C.; Delangle, P. Femtomolar Ln(III) Affinity in Peptide-Based Ligands Containing Unnatural Chelating Amino Acids. *Inorg. Chem.* **2012**, *51*, 5458−5464.
(17) Bertini, I.; Gelis, I.; Katsaros, N.; Luchinat, C.; Provenzani, A. Tuning the Affinity for Lanthanides of Calcium Binding Proteins. *Biochemistry* **2003**, *42*, 8011−8021.
(18) Eliseeva, S. V.; Bunzli, J.-C. G. Lanthanide Luminescence for Functional Materials and Bio-Sciences. *Chem. Soc. Rev.* **2010**, *39*, 189−227.
(19) Bunzli, J.-C. G. Lanthanide Luminescence for Biomedical Analyses and Imaging. *Chem. Rev.* **2010**, *110*, 2729−2755.
(20) Louie, A. Multimodality Imaging Probes: Design and Challenges. *Chem. Rev.* **2010**, *110*, 3146−3195.
(21) Mcmurry, T. J.; Raymond, K. N.; Smith, P. H. Molecular Recognition and Metal-Ion Template Synthesis. *Science* **1989**, *244*, 938−943.
(22) Tsukube, H.; Shinoda, S. Lanthanide Complexes in Molecular Recognition and Chirality Sensing of Biological Substrates. *Chem. Rev.* **2002**, *102*, 2389−2403.
(23) Chan, K.W.-Y.; Wong, W.-T. Small Molecular Gadolinium(III) Complexes as MRI Contrast Agents for Diagnostic Imaging. *Coord. Chem. Rev.* **2007**, *251*, 2428−2451.
(24) Taratula, O.; Dmochowski, I. J. Functionalized 129Xe Contrast Agents for Magnetic Resonance Imaging. *Curr. Opin. Chem. Biol.* **2010**, *14*, 97−104.
(25) Selivanova, N. M.; Galeeva, A. I.; Vandyukov, A. E.; Galyametdinov, Yu.G. New Liquid-Crystalline Complex C_{12}DMAO/LaIII with the Nematic Phase. *Russ. Chem. Bull.* **2010**, *59*, 469−472.
(26) *HyperChem 8.07*; Hypercube, Inc.: Gainesville, FL, 2009 (http://www.hyper.com).
(27) Allinger, N. L. Conformational analysis. 130. MM2. A Hydrocarbon Force Field Utilizing V1 and V2 Torsional Terms. *J. Am. Chem. Soc.* **1977**, *99*, 8127−8134.
(28) Selivanova, N. M.; Osipova, V. V.; Strelkov, M. V.; Manyurov, I. R.; Galyametdinov, Yu. G. Geometric Characteristics of Micellar Systems as Precursors of Lanthanide-Containing Lyotropic Mesophases. *Russ. Chem. Bull.* **2007**, *56*, 56−61.
(29) Parker, C. A. *Photoluminescence of Solutions*; Elsevier: Amsterdam, London, New York, 1968.
(30) Rusanov, A. I. *Micelle Formation in Solutions of Surfactants*; Khimiya: St. Petersburg, Russia, 1992.
(31) Corrin, M. L.; Harkins, W. D. The Effect of Salts on the Critical Concentration for the Formation of Micelles in Colloidal Electrolytes. *J. Am. Chem. Soc.* **1947**, *69*, 683−688.
(32) Shinoda, K.; Nakachava, T.; Tamasurn, B. *Colloidal Surfactants*; World: Moscow, 1966.
(33) Selivanova, N. M.; Osipova, V. V.; Galyametdinov, Yu. G. Effect of a Lanthanide Ion on the Micellation and Self-Organization of Lyotropic Liquid Crystal Systems. *Russ. J. Phys. Chem. A* **2006**, *80*, 649−653.
(34) Zhang, G.; Chen, X.; Xie, Y.; Zhao, Y.; Qiu, H. Lyotropic Liquid Crystalline Phases in a Ternary System of 1-Hexadecyl-3-Methylimidazolium Chloride/1-Decanol/Water. *J. Colloid Interface Sci.* **2007**, *315*, 601−606.
(35) Stilbs, P. Fourier Transform Pulsed-Gradient Spin-Echo Studies of Molecular Diffusion. *Prog. Nucl. Magn. Reson. Spectrosc.* **1987**, *19*, 1−45.
(36) Soderman, O.; Stilbs, P. NMR Studies of Complex Surfactant Systems. *Prog. Nucl. Magn. Reson. Spectrosc.* **1994**, *26*, 445−482.
(37) Jansson, M.; Stilbs, P. A Comparative Study of Organic Counterion Binding to Micelles with the Fourier Transform NMR Self-Diffusion Technique. *J. Phys. Chem.* **1985**, *89*, 4868−4873.
(38) Wasserman, A. M. Spin Probes in Micelles. *Russ. Chem. Rev.* **1994**, *63*, 391−401.
(39) Zangger, K.; Respondek, M.; Gobl, C.; Hohlweg, W.; Rasmussen, K.; Grampp, G.; Madl, T. Positioning of Micelle-Bound Peptides by Paramagnetic Relaxation Enhancements. *J. Phys. Chem. B* **2009**, *113*, 4400−4406.
(40) Miura, T.; Kageyama, A.; Torii, S.; Murai, H. Photoreactions and Molecular Dynamics of Radical Pairs in a Reversed Micelle Studied by Time-Resolved Measurements of EPR and Magnetic Field Effect. *J. Phys. Chem. B* **2010**, *114*, 14550−14558.
(41) Hellmich, U. A.; Lyubenova, S.; Kaltenborn, E.; Doshi, R.; Veen, H. W.; Prisner, T. F.; Glaubitz, C. Probing the ATP Hydrolysis Cycle of the ABC Multidrug Transporter LmrA by Pulsed EPR Spectroscopy. *J. Am. Chem. Soc.* **2012**, *134*, 5857−5862.
(42) Nuti, L.; Ottaviani, M. F. Interaction of Manganese(II) with Pyridine and Poly(2-Vinylpyridine) in Ethanol Solution Studied by Electron Spin Resonance. *J. Phys. Chem.* **1985**, *89*, 4773−4778.
(43) Tummino, P. J.; Gafni, A. Determination of the Aggregation Number of Detergent Micelles Using Steady-State Fluorescence Quenching. *Biophys. J.* **1993**, *64*, 1580−1587.
(44) Prieto, F. R.; Rodriguez, M. C. R.; Gonzalez, M. M.; Rodriguez, A. M. R.; Fernandez, J. C.M. Fluorescence Quenching in Micro-heterogeneous Media. *J. Chem. Educ.* **1995**, *72*, 662−663.
(45) Mathias, J. H.; Rosen, M. J.; Davenport, L. Fluorescence Study of Premicellar Aggregation in Cationic Gemini Surfactants. *Langmuir* **2001**, *17*, 6148−6154.
(46) Duhamel, J. New Insights in the Study of Pyrene Excimer Fluorescence to Characterize Macromolecules and their Supramolecular Assemblies in Solution. *Langmuir* **2012**, *28*, 6527−6538.
(47) Dévédec, F. L.; Fuentealba, D.; Strandman, S.; Bohne, C.; Zhu, X. X. Aggregation Behavior of Pegylated Bile Acid Derivatives. *Langmuir* **2012**, *28*, 13431−13440.
(48) Pan, A.; Naskar, B.; Prameela, G. K. S.; Phani Kumar, B. V. N.; Mandal, A. B.; Bhattacharya, S. C.; Moulik, S. P. Amphiphile Behavior in Mixed Solvent Media I: Self-Aggregation and Ion Association of Sodium Dodecylsulfate in 1,4-Dioxane−Water and Methanol−Water Media. *Langmuir* **2012**, *28*, 13830−13843.
(49) Graciani, M. M.; Rodríguez, A.; Martín, V. I.; Moyá, M. Lu. Micellization and Micellar Growth of Alkanediyl-α,ω-bis-(Dimethyldodecylammonium Bromide) Surfactants in the Presence of Medium-Chain Linear Alcohols. *J. Colloid Interface Sci.* **2010**, *342*, 382−391.
(50) Singh, S. K.; Bajpai, M.; Tyagi, V. K. Amine Oxides: A Review. *J. Oleo Sci.* **2006**, *55*, 99−119.
(51) Yatsimirskii, K. B.; Kostromina, N. A.; Sheka, Z. A.; Devidenko, N. K.; Kriss, E. E.; Ermolenko, V. I. *Khimiya Kompleksnykh Soedinenii Redkozemel'Nykh Elementov (Coordination Chemistry of Rare Earth Elements)*; Naukova Dumka: Kiev, Russia, 1966.